AGU PUBLICATIONS

JGR

Journal of Geophysical Research: Earth Surface

RESEARCH ARTICLE
10.1002/2014JF003169

Key Points:
- Colorado River terraces and tributary long profiles record salt deformation
- Rapid incision supports connection between local unloading and salt deformation
- Incision rate pattern marks transient signal, perhaps from river integration

Supporting Information:
- Text S1
- Figures S1 and S2
- Tables S1 and S2

Correspondence to:
J. L. Pederson,
joel.pederson@usu.edu

Citation:
Jochems, A. P., and J. L. Pederson (2015), Active salt deformation and rapid, transient incision along the Colorado River near Moab, Utah, *J. Geophys. Res. Earth Surf.*, *120*, 730–744, doi:10.1002/2014JF003169.

Received 8 APR 2014
Accepted 18 MAR 2015
Accepted article online 23 MAR 2015
Published online 22 APR 2015

Active salt deformation and rapid, transient incision along the Colorado River near Moab, Utah

Andrew P. Jochems[1,2] and Joel L. Pederson[1]

[1]Department of Geology, Utah State University, Logan, Utah, USA, [2]New Mexico Bureau of Geology and Mineral Resources, Socorro, New Mexico, USA

Abstract In certain settings, erosion is driven by and balanced with tectonic uplift, but the evolution of many landscapes is dominated by other factors such as geologic substrate, drainage history, and transient incision. The Colorado Plateau is an example where these controls are debated and where salt deformation is hypothesized to be locally active and driven by differential unloading, although this is unconfirmed and unquantified in most places. We use luminescence-dated Colorado River terraces upstream of Moab, Utah, to quantify rates of salt-driven subsidence and uplift at the local scale. Active deformation in the study area is also supported by patterns of concavity along tributary drainages crossing salt structures. Subsidence in Professor Valley at a time-averaged rate of ~500 m/Myr (meters/million years) is superimposed upon rapid bedrock incision rates that increase from ~600 to ~900 m/Myr upstream through the study area. Such high rates are unexpected given the absence of sources of regional tectonic uplift here. Instead, the incision rate pattern across the greater area is consistent with a transient signal, perhaps still from ancient drainage integration through Grand Canyon far downstream, and then amplified by unloading at both the broad regional scale and at the local canyon scale.

1. Introduction

It is intuitive that rapid erosion and steep topography are the products of active tectonic uplift, and work by some of the first geologists to study the American West interpreted the Colorado Plateau's youthful-appearing canyon landscape as a classic example of these expectations [*Powell*, 1875; *Davis*, 1901]. Broad research over the past few decades has indeed established relations between erosion, topography, and isostatic feedback in the effort to decipher tectonics from topography, especially in the most tectonically active landscapes [e.g., *Molnar and England*, 1990; *Merritts and Ellis*, 1994; *Pazzaglia and Knuepfer*, 2001; *Whipple*, 2004]. Despite the profound influence of these studies, most of Earth's landscapes lie away from active tectonic margins, and simple relations between uplift and topography are often masked by other factors. One example is how base-level fall associated with drainage integration/capture can create complex, long-lived erosion histories [*Zaprowski et al.*, 2001; *Schoenbohm et al.*, 2004; *Cook et al.*, 2009; *Prince et al.*, 2011].

The Colorado Plateau is an example of such a transient landscape where the rates and drivers of deformation and incision are undergoing renewed debate. Some workers have interpreted mantle sources of dynamic support along the margins of the plateau and have linked these to patterns of incision [*Karlstrom et al.*, 2008; *van Wijk et al.*, 2010; *Levander et al.*, 2011; *Darling et al.*, 2012; *Karlstrom et al.*, 2012]. Yet those potential sources have modest uplift rate estimates and match neither the spatial pattern of deep, late Cenozoic exhumation [*Flowers et al.*, 2008; *Roy et al.*, 2009; *Hoffman et al.*, 2011; *Lazear et al.*, 2013; *Lee et al.*, 2013] nor late Pleistocene river incision [*Pederson et al.*, 2013a], both focused in the central plateau. In fact, some of the only late Cenozoic deformation in the Colorado Plateau relates not to traditional tectonics but to subsurface salt movement documented in the ancestral Paradox Basin [*Case and Joesting*, 1972; *Trudgill*, 2011]. There is evidence that this smaller-scale deformation has been recently active [*Colman*, 1983; *Doelling et al.*, 1988; *Guerrero et al.*, 2015], but such Quaternary movement in most places is unconfirmed and unquantified. Any renewed salt deformation is hypothetically driven by differential unloading from canyon incision and then dissolution and thus may link back to the erosional history of this landscape.

River terraces and longitudinal profiles provide markers in the landscape for measuring deformation and addressing potential salt-related motion. With chronologic constraints, surveyed terraces are especially useful for the study of incision rates and regional patterns of deformation [e.g., *Merritts et al.*, 1994; *Burbank*

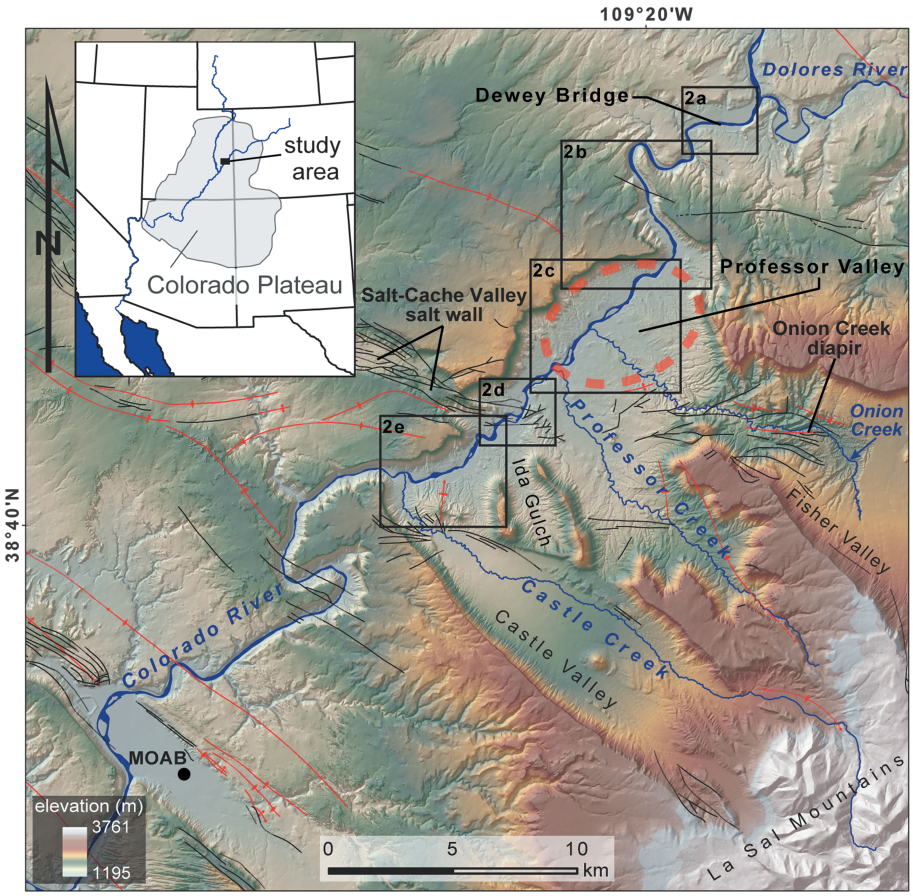

Figure 1. Study area of Colorado River and tributaries in the northcentral Colorado Plateau. Locations of salt structures are indicated, with the aligned Salt Cache Valley structure and Fisher Valley, as well as Castle Valley located where salt walls of the Paradox Formation extend to the surface. The black lines are the normal faults, the red lines are the folds, and the dashed orange ellipse is the area of greatest subsidence recorded in deformation of terraces. The black frames show locations of study reaches identified in Figures 2a–2e.

et al., 1996; *Pazzaglia and Brandon*, 2001]. However, incision rates from fluvial records must be correctly averaged over the time scale of the climate oscillations that create terraces in order to avoid the recognized effect of time scale on those rates and to be representative of base-level controls [*Gardner et al.*, 1987; *Wegmann and Pazzaglia*, 2002; *Pederson et al.*, 2006; *Finnegan et al.*, 2014]. Regarding quantitative methods applied at the broader catchment scale, hypsometry and related topographic metrics have been used to explore geomorphic signatures of tectonic controls [e.g., *Strahler*, 1952; *Frankel and Pazzaglia*, 2006]. Likewise, numerical analysis of the long profiles of streams has been instrumental in revealing spatial and temporal patterns of uplift and the evolution of base level [e.g., *Whipple and Tucker*, 1999; *Snyder et al.*, 2000; *Wobus et al.*, 2006; *Kirby and Whipple*, 2012]. We have applied these valuable approaches to salt tectonic deformation for the first time.

We focus on a section of the Colorado River above Moab, Utah, with well-preserved river terraces and where the main stem Colorado and its tributaries cross known salt tectonic features (Figure 1). Our goals are to document any late Quaternary deformation, calculate the first well-constrained incision rates in this region, and identify topographic signatures that may be broadly useful in signifying salt tectonism. We set our results in the context of what controls the form of this fluvial terrace record as well as the patterns of incision in this highly debated region. The results confirm a diversity of active salt deformation as well as unexpectedly rapid incision by the Colorado River, supporting the hypothesis that incision is driving salt deformation. In the absence of active tectonic uplift in the immediate region, long-lived, transient base-level signals from far downstream and isostatic feedback are likely causes for these dynamics.

2. Background

2.1. Colorado Plateau Landscape Evolution

The Colorado Plateau's high elevation (~2 km), distinctively minor internal deformation, and deep erosion beg explanation, but the history of uplift and erosion throughout the Cenozoic continues to be debated. Sources of epeirogenic rock uplift that have been proposed recently include warming of heterogeneous lithosphere [*Roy et al.*, 2009], lithospheric delamination [*van Wijk et al.*, 2010; *Levander et al.*, 2011; *Karlstrom et al.*, 2012], dynamic support from asthenospheric flow [*Moucha et al.*, 2009], and flexural rebound in response to erosional unloading [*Pederson et al.*, 2002; *Lazear et al.*, 2013]. These distinct hypotheses each have contrasting predictions for the timing and patterns of late Cenozoic uplift in the Colorado Plateau, and there is not enough total uplift to accommodate all of these sources [*Pederson et al.*, 2002].

Although uplift hypotheses are difficult to test, more concrete debate has been focused on spatial and temporal patterns of erosion and river incision in the Colorado Plateau. A pattern of erosional exhumation being younger toward the center of the plateau has been confirmed by U-Th/He thermochronologic data [*Flowers et al.*, 2008; *Hoffman et al.*, 2011; *Lee et al.*, 2013]. This involves a dome of isostatic rebound that acts as a feedback to broad exhumation [*Roy et al.*, 2009; *Lazear et al.*, 2013]. *Pederson et al.* [2013a] identified a concordant bull's eye pattern of rapid late Pleistocene river incision focused in the central plateau. Yet tomography reveals only cold, dense upper mantle beneath the central plateau [*Schmandt and Humphreys*, 2010], and there are no known or proposed sources of surface uplift there. This supports the counterargument that instead of mantle-driven uplift, patterns of erosion and topography are controlled by drainage history, varying bedrock erodability, and amplification by isostatic rebound [*Pederson and Tressler*, 2012; *Pederson et al.*, 2013a].

Researchers have also uncovered patterns of time-variable (i.e., transient) incision in the plateau. *Darling et al.* [2012] interpreted an increase in Colorado River incision rates in the Glen Canyon area, attributing it to a wave of incision migrating upstream of Grand Canyon sometime after ~500 ka. Similarly, *Cook et al.* [2009] found evidence for an increase in main stem incision rates based on oversteepened profiles and cosmogenic dating of terrace gravels of Trachyte Creek, a tributary to the Colorado draining the Henry Mountains in southern Utah. They suggested that this pulse of incision relates to both upstream migration of a base-level signal and its interactions with varying lithology, recognizing that its signal is likely to be found farther upstream in the Colorado River system. Likewise, *Pederson and Tressler* [2012] suggested that there are major potential transient knickzones along the main stem drainage in the northcentral Colorado Plateau.

2.2. Salt Tectonism of the Ancestral Paradox Basin

Late Paleozoic strata of the central Colorado Plateau include great thicknesses of Pennsylvanian evaporites accumulated in the ancestral Paradox Basin flanking the Uncompahgre uplift. Passive deformation induced by subsequent episodes of sedimentation and unloading has resulted in NW-SE trending faults and folds [*Doelling et al.*, 1988], salt walls (elongate, stock-like structures trending along basement faults) reaching 4500 m below the surface in places [*Trudgill*, 2011], and diapirs and ring-faulted collapse centers [*Gutiérrez*, 2004]. These features are commonly associated with arcuate-to-parallel normal faulting in and around the study area (Figure 1). Previous workers have identified multiple episodes of salt-related tectonism since the early Mesozoic based on stratigraphic architecture, including possible phases of activity during the Quaternary [e.g., *Colman*, 1983; *Doelling et al.*, 1988; *Trudgill*, 2011]. Younger salt deformation is typically attributed to dissolution and transport by near-surface waters and, ultimately, differential unloading from canyon cutting by the Colorado River system [*Cater*, 1970; *Huntoon*, 1982; *Gutiérrez*, 2004; *Guerrero et al.*, 2015]. For example, ~125 km downstream of our study area, the Needles fault zone represents gravity-driven deformation above salt bodies into the free boundary of the Colorado River's canyon [*Huntoon*, 1982], and interferometric synthetic aperture radar measurements reveal ongoing deformation [*Furuya et al.*, 2007].

In our study area, the Colorado River flows south through the constricted but low-gradient Dewey Bridge and Dewey Canyon reaches and then opens into the broad Professor Valley (Figure 1). Here the river is joined by tributaries that add coarse debris and create small rapids increasing the river gradient and then the river intersects and crosses the Cache Valley graben, which is key to our research design. Evidence for Quaternary salt activity in the area includes deformation of the Bishop ash (0.76 Ma) observed in small sinkholes along Onion Creek and in Salt Valley [*Colman*, 1983; *Doelling et al.*, 1988]. In the Onion Creek diapir, high mid-Pleistocene erosion rates and a history of drainage reorganization have been attributed to diapiric uplift, potentially

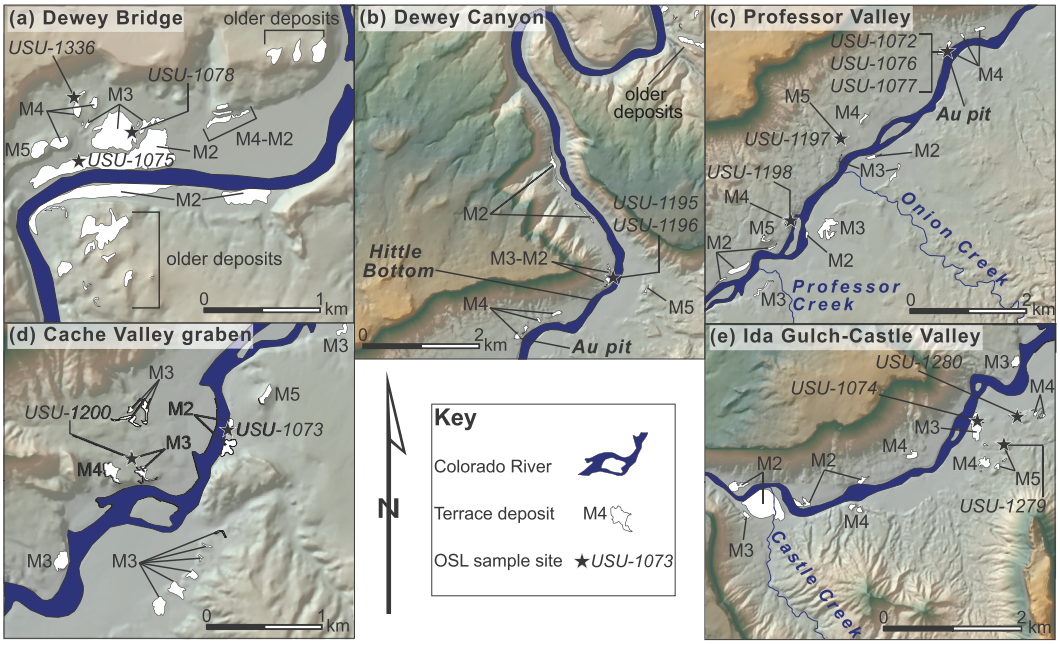

Figure 2. Study reaches of the Colorado River, with late Pleistocene terrace deposits (modified from *Doelling* [2001]) and OSL sample locations. "M" stands for main stem Colorado River terrace deposit (e.g., M2). Note different scales for each reach. The most complete terrace suites are found at (a) Dewey Bridge and (b) Ida Gulch-Castle Valley. Some of the labeled samples were taken at locations with isolated deposits not visible in maps of these scales.

ending ~250 ka [*Colman*, 1983; *Balco and Stone*, 2005]. Beyond this older Quaternary salt activity, deformation in the study area is speculative, with *Colman* [1983] suggesting possible warping of Colorado River terraces on the upstream margin of the Cache Valley graben.

3. Methods

3.1. Terrace Chronostratigraphy

Previous geologic mapping upstream of Moab has identified between four and eight Colorado River terraces throughout the study area [*Doelling*, 1996; *Doelling and Ross*, 1998; *Doelling*, 2002]. This study focused on detailing the extent, form, and elevation of terrace deposits, defining their chronostratigraphy, and correlating terraces across study reaches (Figure 2). We surveyed and correlated four late Pleistocene Colorado River terrace deposits, with elevations documented using real-time kinematic GPS (vertical errors of $\leq$3 cm) and correlation based on physical tracing, landscape position, and terrace depositional ages from optically stimulated luminescence (OSL). Summary elevation data for each deposit is given in Table S1 in the supporting information. (Supporting information are available in the HyperText Markup Language doi:10.1002/2014JF003169.)

Optically stimulated luminescence dating is a burial dating technique that determines the amount of time since sediment grains were last exposed to light during transport [*Huntley et al.*, 1985] and therefore constrains depositional episodes associated with lateral planation of strath terraces or aggradation of fill terraces. Intervening episodes of incision are inferred between dated deposits (see supporting information for full OSL results). Sediment samples of fine-grained to medium-grained, quartz-rich sand with primary sedimentary structures and no indication of bioturbation or soil development were collected along five reaches of the Colorado River (Figure 2). Samples were collected in opaque containers from at least 1 m below the local geomorphic surface (typically the terrace tread). Samples were processed and analyzed following standard laboratory procedures to separate and purify quartz grains for analysis and measured on Risø TL/OSL-DA-20 readers following the single-aliquot regenerative-dose protocol [*Murray and Wintle*, 2000]. Examples of the robust optical properties typical of these samples are shown in Figure S1 in the supporting information.

Table 1. Colorado River Terrace OSL Geochronology

Deposit[a]	Location	Sample No.	Latitude/Longitude[b]	Elevation (m)	# Aliquots (Total)	Dose Rate (Gy kyr^{-1})	Equivalent Dose (Gy)	OD (%)[c]	OSL Age (ka)[d]
M2	Dewey Bridge	USU-1075	38.81°N, 109.31°W	1260	19 (41)	3.42 ± 0.19	104.33 ± 11.38	18.2	30.5 ± 4.5
M2	Cache Valley graben	USU-1073	38.71°N, 109.39°W	1237	17 (30)	2.81 ± 0.15	71.85 ± 11.06	27.9	25.6 ± 4.7
M3	Dewey Bridge	USU-1078	38.67°N, 109.30°W	1273	20 (43)	3.54 ± 0.51	118.78 ± 17.35	27.7	33.6 ± 7.5
M3	Hittle Bottom	USU-1196	38.76°N, 109.32°W	1265	19 (38)	3.30 ± 0.18	94.99 ± 12.82	27.1	28.8 ± 4.8
M3	Hittle Bottom	USU-1195	38.76°N, 109.32°W	1253	20 (27)	3.56 ± 0.19	130.38 ± 13.99	21.5	36.7 ± 5.4
M3	Ida Gulch	USU-1074	38.69°N, 109.41°W	1251	17 (30)	3.25 ± 0.17	129.74 ± 21.32	30.1	39.9 ± 7.7
M4	Dewey Bridge	USU-1336	38.82°N, 109.31°W	1288	19 (36)	3.12 ± 0.16	159.98 ± 27.25	34.3	51.3 ± 10.1
M4	Professor Valley	USU-1072	38.76°N, 109.34°W	1265	21 (36)	3.00 ± 0.16[e]	145.77 ± 24.15	35.7	~49[e] ± NA
M4	Professor Valley	USU-1076	38.75°N, 109.34°W	1258	17 (28)	3.21 ± 0.17	159.92 ± 21.23	24.5	49.9 ± 8.3
M4	Professor Valley	USU-1077	38.75°N, 109.34°W	1256	20 (30)	3.13 ± 0.26	156.23 ± 26.08	34.3	49.9 ± 10.2
M4	Professor Valley	USU-1198	38.73°N, 109.37°W	1284	19 (34)	2.71 ± 0.18	120.67 ± 21.13	36.0	44.5 ± 9.2
M4	Cache Valley graben	USU-1200	38.71°N, 109.40°W	1273	23 (45)	3.15 ± 0.17	157.64 ± 37.09	28.8	50.0 ± 12.8
M4	Ida Gulch	USU-1280	38.69°N, 109.41°W	1264	18 (40)	3.40 ± 0.19	199.74 ± 17.88	16.0	58.7 ± 7.9
M5	Professor Valley	USU-1197	38.75°N, 109.36°W	1307	19 (41)	2.65 ± 0.14	186.42 ± 38.42	38.7	70.4 ± 16.1
M5	Ida Gulch	USU-1279	38.69°N, 109.41°W	1294	18 (38)	2.64 ± 0.14	176.75 ± 40.12	46.2	66.9 ± 16.6

[a]Organized by stratigraphic and long profile position; M stands for main stem Colorado River deposit.
[b]NAD83.
[c]Overdisperion or the percentage of equivalent dose scatter. Included in equivalent dose error.
[d]Reported ages with 2σ error.
[e]Mean dose rate of all Professor Valley samples used due to erroneously high U concentration. Age is only an estimate.

The luminescence signal accrues through natural radiation from the decay of U, Th, Rb, and K, as well as cosmic radiation, and environmental dose rates were determined from sediment surrounding the sample (see Table S1 in the supporting information). Representative dose rate samples were collected within a 30 cm radius of each OSL sample, and elemental concentrations were determined through mass spectrometry. Dose rate conversions for U, Th, Rb, K, and H_2O attenuation follow *Guérin et al.* [2011], and ages were calculated using the central age model of *Galbraith et al.* [1999]. The luminescence age is calculated as the amount of radiation; the sample was exposed to during burial (the equivalent dose) divided by the dose rate. Age distributions are shown in Figure S2 in the supporting information.

Besides dose rate error due to the influence of bioturbation and pedogenesis (mitigated by sampling >1 m below the geomorphic surface and away from soils), luminescence age errors in fluvial deposits may result from partial bleaching, the tendency for the luminescence signal to be incompletely reset in rivers with large, sunlight-blocking suspended sediment loads [*Murray and Olley*, 2002]. However, the effects of partial bleaching are expected to be diminished by the large equivalent doses determined for late Pleistocene deposits [*Murray and Olley*, 2002; *Rittenour*, 2008], which mostly exceed 100 Gy in the study area (Table 1). Total 2σ errors on luminescence ages include random and systematic errors from equivalent dose scatter (overdispersion), uncertainties in the calculation of environment dose rates, and instrumental error (Table 1).

3.2. Terrain Analyses

Terrain analyses were performed on 10 m digital elevation models using ArcGIS and MATLAB tools described in *Wobus et al.* [2006] (available at http://www.geomorphtools.org/), which quantify a normalized steepness index (k_{sn}) and reach-scale concavity (θ) along tributary long profiles. The normalized steepness index is a generalized form of *Hack*'s [1973] stream-gradient index that allows steepness comparison between drainages and identification of anomalies/knickpoints based on a reference profile concavity, θ_{ref}. The calculation of overall profile concavity and k_{sn} assumes that the river profile is in steady state with respect to uplift and climate and that uplift rate and erosivity are uniform throughout each reach [*Snyder et al.*, 2000]. Derivation of k_{sn} is described in detail elsewhere [*Whipple and Tucker*, 1999; *Snyder et al.*, 2000; *Wobus et al.*, 2006; *Kirby and Whipple*, 2012] and is given as a normalized version of Flint's law:

$$s = k_{sn} A^{-\theta_{ref}}, \quad (1)$$

where S is the slope and A is the upstream drainage area [*Flint*, 1974; *Howard*, 1994]. The chosen value of θ_{ref} is based on the characteristic concavity of stream profiles and is typically 0.4–0.6 in steady state landscapes [*Wobus et al.*, 2006]. In our three study area tributaries, reach concavity was first calculated independently,

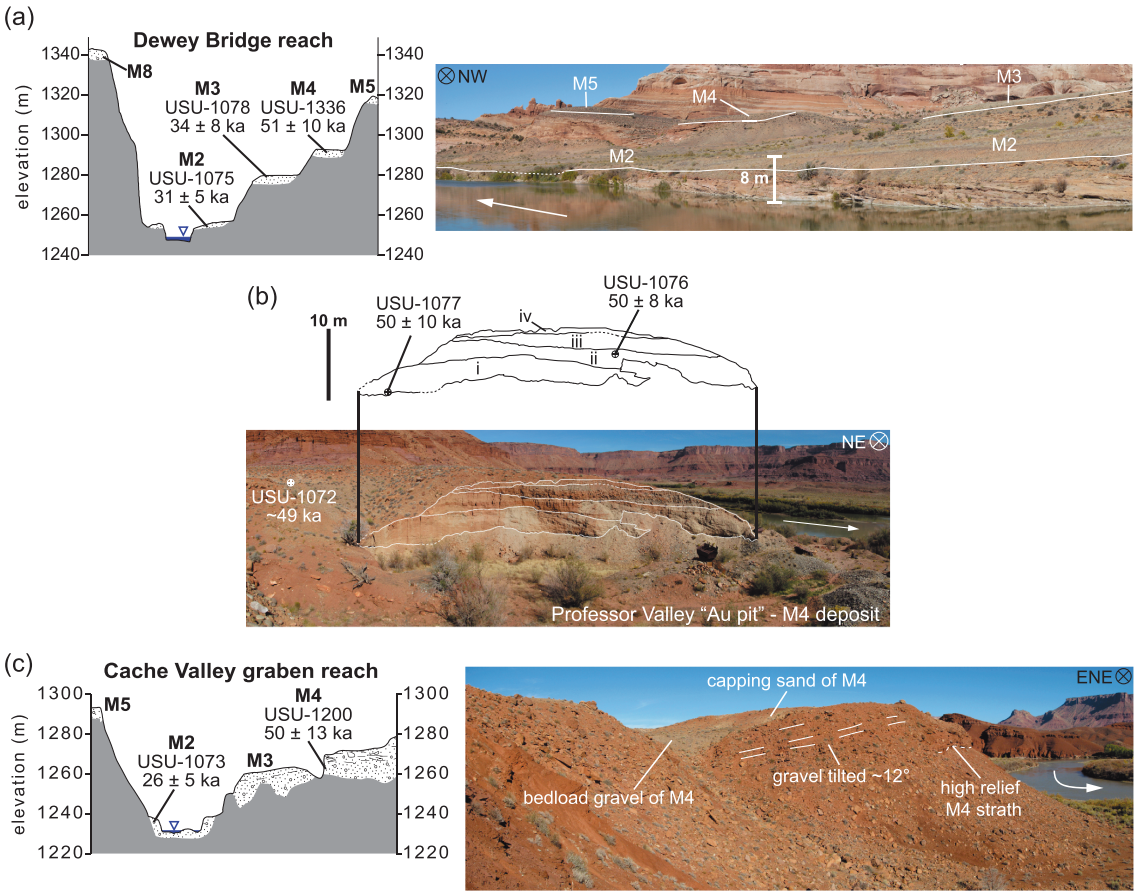

Figure 3. Reach-scale changes in terrace morphology throughout the study area. (a) Dewey Bridge reach cross section with local OSL age constraints and annotated photograph looking downstream at planar strath terraces (average deposit thickness = 4.3 m) located at the upstream end of the study area. (b) Photograph with annotated stratigraphy of the contrasting, >10 m thick M4 deposit at the Professor Valley placer gold mine locality. Basal bed load gravel is exposed in northeast facing wall of pit (not shown), and units I and II are interpreted as channel margin sandbar deposits with minor interfingering of piedmont alluvium; unit III is gravel bar/bed load deposits, and unit IV is piedmont debris flow deposit. (c) Cache Valley graben reach cross section with local OSL ages and photograph illustrating tilting of basal M4 gravels into sinkhole and undeformed, infilling deposits.

and then, based upon the average concavity of upper drainage reaches insulated from base-level fall, we set $\theta_{ref} = 0.35$ and k_{sn} values were calculated (with units of $m^{0.7}$ in our case). Long profiles were smoothed with a moving-average window of 250 m, and elevation values were extracted at 10 m contours, whereas stream gradient for all k_{sn} calculations was derived at contour intervals of 12.192 m (40 ft).

4. Results

4.1. Correlation and Deformation of Colorado River Terraces

Although a few higher terrace remnants exist, four primary terrace levels (M5-M2; M for "main stem") are documented in detail across the study reaches, with 15 OSL ages determined for this flight of younger deposits (Figure 2) [*Jochems*, 2013]. Correlations for older remnants, including M5 and M4, are challenging because terraces along the central river profile are indeed deformed, and the age of certain deposits may be influenced by the timing of localized subsidence. Thus, we more heavily weigh our results regarding the easily traced younger M3 and M2 terraces. Our confidence in this chronostratigraphy is also informed by correspondences to two comparable records in the northcentral plateau, along the Green River at Crystal Geyser to the west [*Pederson et al.*, 2013b] and along the Colorado River upstream near Grand Junction, Colorado [*Aslan and Hanson*, 2009]. Overall, we found that OSL ages of this suite of terrace deposits span the last ~75 kyr, with episodes of deposition at ~75–65 ka for the M5, ~60–45 ka for the M4, ~40–35 ka for the M3, and ~30–25 ka for the M2 (Table 1).

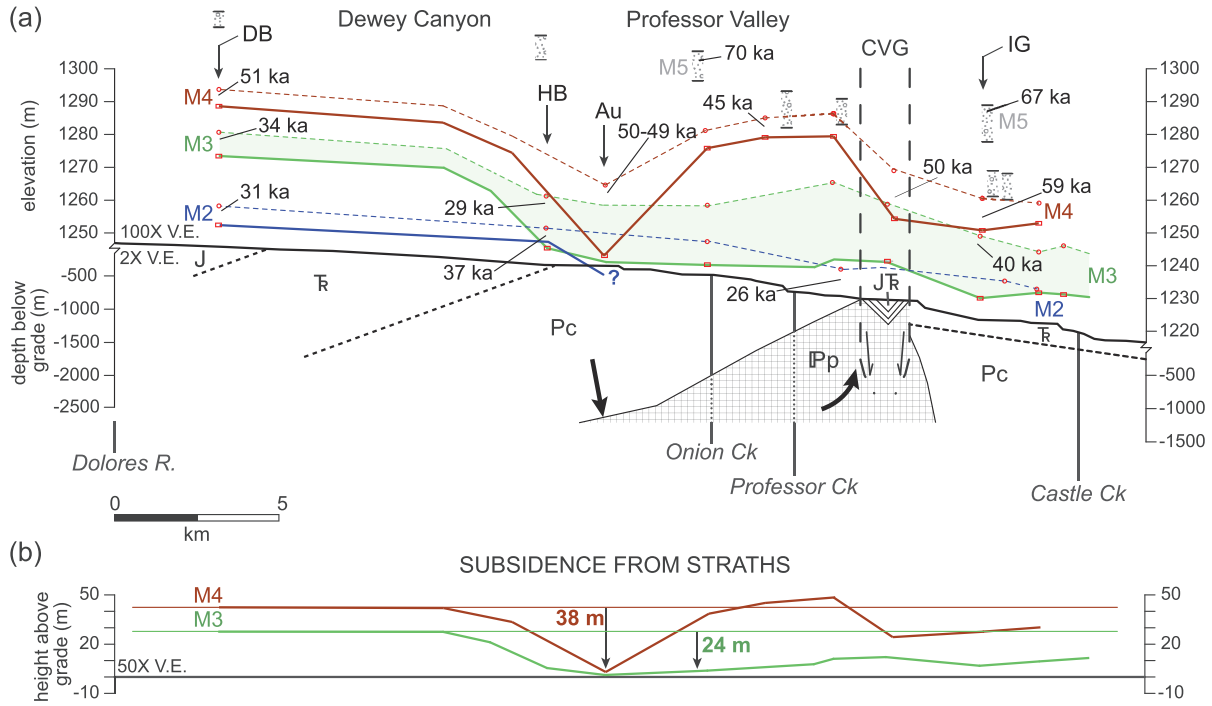

Figure 4. Colorado River terrace correlations and deformation in longitudinal profile. (a) Long profile with underlying bedrock through study reaches (note different subsurface scale). Geologic units: J–Jurassic, T_R–Triassic, Pc–Permian Cutler Group, and IPp–Pennsylvanian Paradox Formation. The M5, M4, M3, and M2 terraces are surveyed at locations of red marks and shown with correlated straths (solid line) and preserved treads (dashed). Note deformation and deposit thickening through Professor Valley and Cache Valley graben (CVG). Central OSL ages labeled at their sample positions (three OSL ages are represented at Au locality). Localities are DB = Dewey Bridge, HB = Hittle Bottom, Au = Professor Valley placer gold mine, and IG = Ida Gulch. (b) M4 and M3 strath profiles normalized relative to river level illustrating deformation.

Two major patterns emerge when surveyed terrace straths and treads are correlated in long profile. First, deposits thicken greatly between the canyon reach at Dewey Bridge (Figure 3a) and the broader downstream reaches across Professor Valley (Figure 3b) and the Cache Valley graben (Figure 3c). At Dewey Bridge are quintessential strath terraces, with an average of 4.3 m of cobbly alluvial cover. Downstream are fill terrace deposits 10–20 m thick, with irregular basal straths and finer-grained sedimentary facies preserved. The M4 is thickest (22 m) at the Professor Valley gold mine locality (Figure 3b), and the preservation of associated fine-grained overbank and channel margin facies indicates that the Colorado River was dominantly aggrading in this location ~60–45 ka. Likewise, the M3 deposit remains ~15 m thicker throughout the lower half of the study area compared to Dewey Bridge, and the M2 is at least 8 m thicker with its strath plunging below grade, with mostly upper sandy facies exposed. The M4 and M3 deposits remain thick through the Cache Valley graben and display high relief on their basal straths (Figure 3c). Also observed in the graben is an approximately 3000 m^2 sinkhole collapse center containing deformed basal M4 gravels and infilled and capped by undeformed M4 overbank deposits.

Using our chronostratigraphy, an approximate subsidence rate can be calculated for Professor Valley terrace deposits relative to terraces upstream. The M4 strath at the "Au" locality is 38 m lower than at Dewey Bridge (Figure 4), and with a basal age for the M4 of ~60 ka, the time-averaged subsidence rate at the Au locality is ~600 m/Myr. A more confident calculation across Professor Valley is derived using the well-preserved M3, which has a strath 24–18 m lower across the downstream study reaches relative to Dewey Bridge (Figure 4). Given a basal age of ~40 ka, this represents ~500 m/Myr (0.5 m/kyr) of time-averaged, relative subsidence in Professor Valley. Additionally, the M2 strath drops at least 5 m (observed height) below grade downstream of Hittle Bottom, implying more than 5 m of subsidence since 30 ka and therefore a more recent time-averaged subsidence estimate of >175 m/Myr (>0.175 m/kyr).

The second pattern observed in the morphology of study area terrace deposits is the uplift and tilting of the straths approaching the Cache Valley graben (Figure 4a). If post-40 ka subsidence recorded by the M3 is restored, deformation of the M4 strath before that time (the envelope between the M4 and M3 lines in Figure 4b)

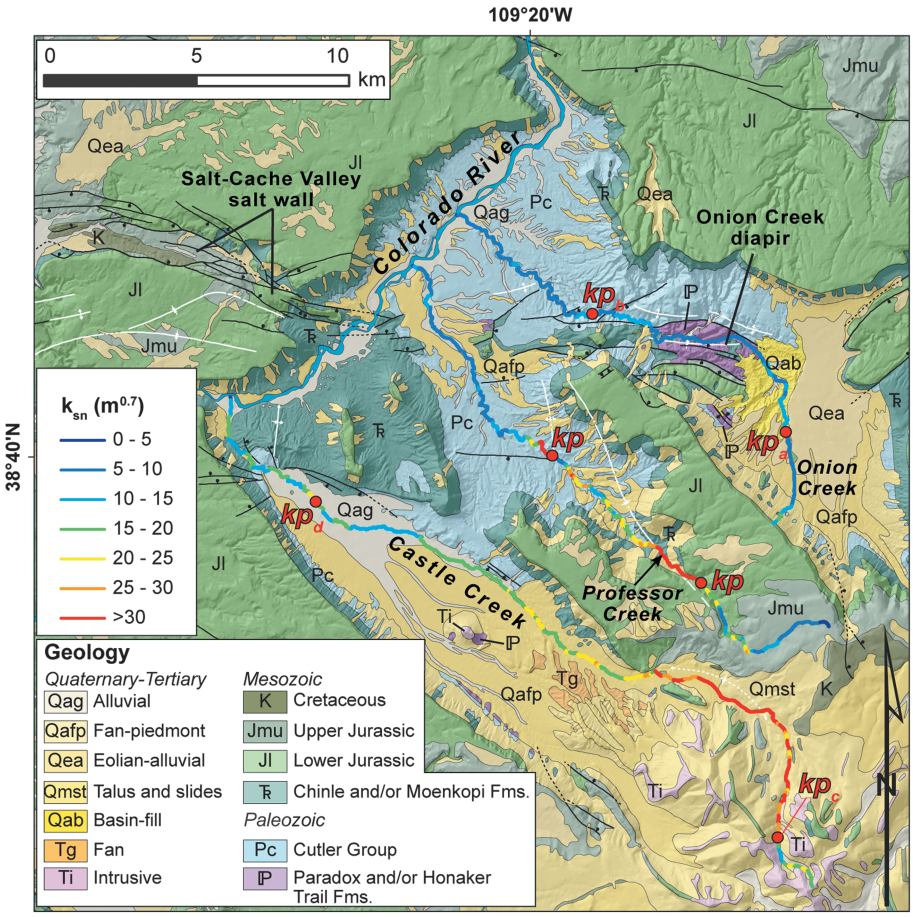

Figure 5. Geologic map of the study area with normalized steepness index (k_{sn}) profiles shown for three Colorado River tributaries. Geology is simplified from *Doelling* [2001]. Cliffs in the study area are formed by resistant Lower Jurassic sandstone (Jl), whereas valleys are underlain by weaker Triassic mudstone (T_R) and Permian Cutler Group conglomerate (Pc). Knickpoints (*kp*) are shown in each profile; knickpoint subscripts in Castle and Onion creeks correspond to those marked in Figure 6. Note that the upper knickpoint in Professor Creek is associated with the downstream transition from resistant, cliff-forming Jurassic sandstone to weaker mudstone of the Triassic Chinle Formation. Castle and Onion creek knickpoints are discussed in text. See Figure 1 for geographic features and landmarks.

reveals apparent tilting upstream off the flank of the Cache Valley graben ~60–40 ka, supporting *Colman*'s [1983] interpretation of the same. This is due to both subsidence in upper Professor Valley and up to 20 m of relative uplift downstream.

4.2. Tributary Signatures of Salt Deformation

In our effort to investigate the utility of terrain analysis for areas of salt deformation, metrics such as the hypsometric integral and basin volume-to-area ratio were calculated for each of the three study area tributaries [*Jochems*, 2013], but long profile analyses of concavity and steepness reveal the clearest differences and are presented here. Each tributary is of similar size/order, connects to the same Colorado River base level, and all three have distinct upper knickpoints and less distinct lower knickpoints. Also for our research design, each has different relations to salt features: Onion Creek transects its diapir, lower Castle Creek longitudinally traverses a salt graben, and Professor Creek does not encounter salt bodies or definitive salt-related structures and thus serves as a control case (Figure 5). Professor Creek's profile is clearly dominated by adjustments to bedrock, with knickpoints distinguishing an upper reach of nearly zero concavity (straight) through Jurassic sandstones and a middle reach dominated by a steep knickzone coinciding with the cliff-forming, Triassic Wingate Sandstone (Figure 5) [*Jochems*, 2013].

Both Onion and Castle creeks have upper knickpoints well above their respective salt bodies and more subtle lower knickpoints near the downstream ends of those features, which are apparent in the field and in k_{sn} data

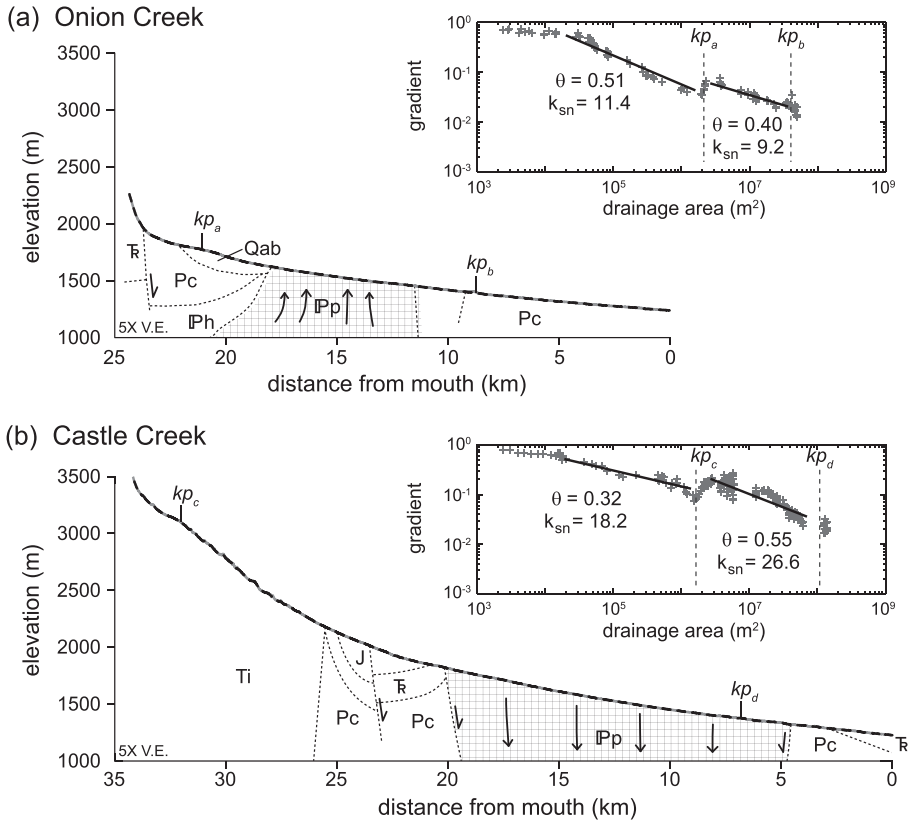

Figure 6. Longitudinal profiles and slope-area plots of tributary drainages crossing salt features. Subsurface geologic units are: Qab–Quaternary basin fill of Fisher Valley, Ti–Tertiary intrusive, J–Jurassic, T_R–Triassic, Pc–Permian Cutler Group, IPh–Pennsylvanian Honaker Trail Formation, and IPp–Pennsylvanian Paradox Formation. Inset slope-area diagrams show nonnormalized reach concavity (θ) and steepness index (k_{sn}) values ($m^{0.7}$) from a best fit regression (dark black lines) for reaches separated by knickpoints (kp) on profiles. A reference concavity of 0.35 was used to calculated k_{sn}. (a) Onion Creek approaches and crosses the uplifting diapir with lower concavity relative to its upper reach. (b) Castle Creek has a steep drainage below the glacial limit and is highly concave approaching and crossing the subsiding Castle Valley salt wall.

but not in slope-area plots (Figures 5 and 6). The relatively low gradient middle reach of Onion Creek approaching and crossing the diapir, between knickpoints kp_a and kp_b in Figure 6a, has a θ of 0.40 (note that θ is the calculated reach concavity and is distinct from θ_{ref}, which is used only in the calculation of k_{sn}). This reach is distinctly less concave than the upper, insulated reach of Onion Creek ($\theta = 0.51$; Figure 6a). The steepness values for the upper and middle Onion Creek reaches are similar, with a mean k_{sn} of the upper reach of 11.4 ± 1.0 and the middle reach a somewhat lower 9.2 ± 0.1 (Figure 6a). Knickpoint kp_a separating these reaches represents an advancing headcut of Onion Creek into erodible basin fill (Figures 5 and 6), deposited in conjunction with middle Pleistocene rise of the Onion Creek diapir [*Colman*, 1983; *Balco and Stone*, 2005]. The less concave profile below this knickpoint may reflect the adjustment of Onion Creek to some degree of ongoing diapiric uplift.

To the south, Castle Creek is steeper (average k_{sn} more than 2 times that of Onion Creek), with an upper knickpoint near the Pleistocene glacial limit in the La Sal Mountains, above a talus-choked knickzone. Castle Creek has an upper reach θ of 0.32 and a greater θ of 0.55 as it exits this knickzone and transitions downstream to low gradients flowing down the Castle Valley graben (Figure 6b). The k_{sn} values for Castle Creek are 18.2 ± 0.3 in the upper, glaciated reach and a steeper 26.6 ± 0.7 in the middle reach.

4.3. Colorado River Incision Rates

To calculate incision rates in the study area, we take the linear trend of base-level fall through the dated and surveyed Colorado River terrace deposits as illustrated chronostratigraphically in Figure 7. This is independent

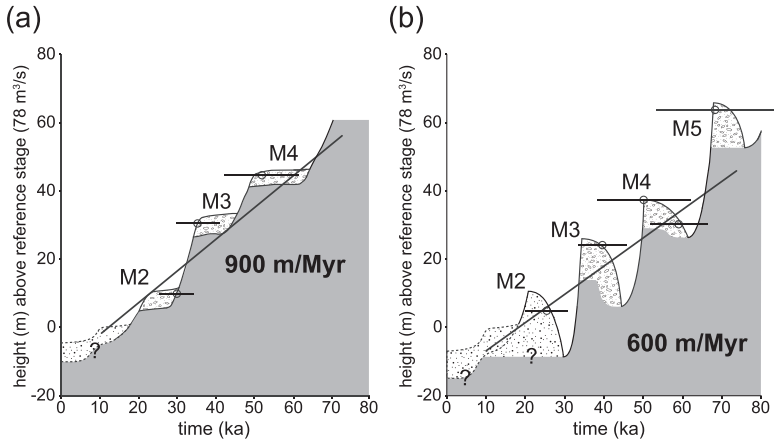

Figure 7. Late Pleistocene Colorado River incision rates from terrace chronostratigraphy. Rates are given by the base-level fall trend through OSL-dated terrace deposits with surveyed height above modern channel (base flow of 78 m^3/s). (a) Dewey Bridge, where there is no evidence for salt deformation and strath terraces record surprisingly fast incision, and (b) Ida Gulch downstream, where thicker fill terraces record somewhat slower incision rates. Local OSL dates are illustrated with 2σ error, whereas the time-width of each terrace deposit reflects range of ages in full data set.

of the modern position of the channel and spans glacial-interglacial climate cycles (marine oxygen isotope stage (MIS) 4 to MIS 2) in order to avoid any "Sadler effect"—the dependence of incision rate on timespan [*Gardner et al.*, 1987; *Finnegan et al.*, 2014]. That is, we avoid the artificially high-rate estimates that can come from using timespans similar to or shorter than the variability or "noise" in the system [e.g., *Jerolmack and Paola*, 2010], by calculating bedrock incision integrated across the climate oscillations that help create the terrace record [*Wegmann and Pazzaglia*, 2002; *Pederson et al.*, 2006]. At Dewey Bridge, upstream of any suspected or observed salt deformation, there is unexpectedly rapid late Pleistocene incision at ~900 m/Myr (0.9 m/kyr) (Figure 7). A slower incision rate of ~600 m/Myr (0.6 m/kyr) is calculated near Ida Gulch, downstream of the deforming Professor Valley and Cache Valley graben reaches.

5. Discussion

5.1. Colorado River Terraces and Their Deformation

Addressing broad issues of how and why terrace records are formed is beyond the scope of our data set, but some observations about patterns in our Colorado River terraces are warranted. It is well established that Pleistocene-scale fluvial terrace records are formed by the effects of climate oscillations that are superimposed upon base-level fall [e.g., *Hancock and Anderson*, 2002; *Wegmann and Pazzaglia*, 2002; *Pederson et al.*, 2006]. This includes both thin strath terraces and fill terraces aggrading in valley bottoms with deposits up to tens of meters thick [e.g., *Bull*, 1990; *Pazzaglia and Brandon*, 2001; *Hancock and Anderson*, 2002; *Pazzaglia*, 2013]. Thus, it is commonly anticipated that Pleistocene fluvial deposits will correlate in age across river systems responding to regional climate forcings. Colorado River M4 and M3 terrace deposits in our study area have a similar chronology as main stem Green River terraces at Crystal Geyser, Utah, where deposits with the same unit designations have been dated at ~60 and ~40 ka using OSL [*Pederson et al.*, 2013b]. Similarly, main stem M5 and M2 deposit ages in the study area overlap in age with Colorado River deposits ~120 km upstream near Grand Junction, Colorado, dated at ~68–64 and ~24 ka using OSL [*Aslan and Hanson*, 2009]. Especially considering that the study localities in our central reaches have the complicating influence of subsidence on the timing of deposition, these rough correlations suggest that Milankovitch-scale climate drivers have effectively operated to form our terrace record. In fact, terrace geometry or form, rather than age, appears to be more strongly influenced by salt deformation in our study area.

The Colorado River across our study area has left a pattern of thin strath terrace deposits in the restricted upper canyon at Dewey Bridge and thicker fill terrace deposits in the unconfined reaches downstream. It is interesting that this is opposite the pattern observed elsewhere in the region away from salt influence [*Pederson et al.*, 2006, 2013b], which aligns with the expectation from other work that thin strath terraces should be found in settings of weak bedrock favorable to lateral planation [e.g., *Montgomery*, 2004;

Finnegan and Balco, 2013], and that climate-induced aggradation of fill terraces is expected in restricted canyons [*Hancock and Anderson*, 2002]. In fact, only thin strath terrace deposits are found in our upper study reaches, which are constricted by steep talus and cliffs of Upper Triassic and Jurassic strata (Figures 2 and 5). Downstream, unexpectedly thick M4, M3, and M2 fill deposits are found in broad Professor Valley, which is underlain by relatively weak sediments of the Permian Cutler Formation and shaley Lower Triassic strata.

Turning to salt deformation of these terrace markers, some of our strongest evidence is this abrupt increase in deposit thickness downstream through the study area, which otherwise defies expectations. We interpret this as a result of syndepositional subsidence at the reach scale, which is equal to or greater than the magnitude of deposit thickening (Figure 4b). The time-averaged subsidence of the M3 deposit across Professor Valley is calculated at ~500 m/Myr, and it seems that subsidence was active over all the episodes of terrace deposition, inasmuch as it increased accommodation for thicker M2, M3, and M4 and even less well preserved M5 deposits in Professor Valley.

The mechanisms responsible for variable, reach-scale subsidence and tilting along the Colorado River are both near-surface dissolution and salt movement at depth. The Cache Valley graben and the Onion Creek diapir bring Paradox evaporites to the surface, and under subsiding Professor Valley, there is also evidence for significant Pennsylvanian salts [e.g., *Doelling et al.*, 1988; *Trudgill*, 2011], but they are stratigraphically ~2 km below the surface (Figure 4a). Our chronostratigraphy shows that there was essentially simultaneous subsidence in Professor Valley and uplift and salt removal (sinkhole collapse in Figure 3c) downstream in the Cache Valley graben during aggradation of the M4 deposit. Thus, we hypothesize that neighboring areas of rising salt 5–10 km south and east in the Cache Valley salt wall and the Onion Creek diapir drew from the formation at depth and lead to subsidence of Professor Valley, perhaps accounting for its distinctly elliptical bowl (Figures 1 and 4).

Our averaged subsidence rate of ~500 m/Myr is reasonable given its similarity to geodetically determined rates in the Needles fault zone to the southwest in the ancestral Paradox Basin [*Furuya et al.*, 2007]. Elsewhere, an analogous pattern of terrace deformation and thickening by evaporite subsidence has been recorded by field studies in the Ebro Basin of Spain [*Gutiérrez*, 1996; *Guerrero et al.*, 2008]. There, upward fining facies in unexpectedly thick deposits resemble the Colorado River Au M4 deposit (Figure 3b). Likewise, Tertiary and Quaternary gravels of the Canadian River in the Texas Panhandle exhibit clear warping and folding due to dissolution of Permian salt facies [*Gustavson*, 1986]. Folding and anomalous patterns in valley-bottom thicknesses of late Pleistocene glacial outwash terraces and overlying debris-flow fans are observed along the Roaring Fork River in western Colorado, resulting from flexural-slip faulting related to evaporite flow in a diapir [*Kirkham et al.*, 2002; *Gutiérrez et al.*, 2014]. Returning to Triassic rocks exposed in the study area, diapirism of Paradox evaporites in southeastern Utah has been recognized as having exerted strong control on deposition of strata of the fluvial Chinle Formation [*Hazel*, 1994]. Thus, the seemingly uncommon phenomenon of salt deformation affecting fluvial processes has been documented (though not necessarily quantified) in other river systems worldwide and constitutes a locally important control on fluvial stratigraphic architecture in both modern and ancient fluvial systems.

5.2. Signatures of Salt Deformation Along Tributary Profiles

In addition to reach-scale changes in Colorado River terraces, we have explored the spatial distribution of knickpoints and patterns of overall stream concavity (θ) along study tributaries as relating to salt deformation (Figures 5 and 6). All three study area tributaries have two knickpoints that, being erosional landforms, ultimately formed due to base-level fall. Yet the position of these particular knickpoints is related to lithologic changes or salt activity, and thus, we recognize that any information they hold regarding the number and timing of transient signals along the Colorado River is obscured. Accordingly, we interpret these topographic signatures in the context of those local controls within the tributaries and as additional evidence for salt deformation.

Both Onion Creek and Castle Creek cross salt structures of known or suspected Quaternary activity, and although their reach changes in k_{sn} are too subtle to be definitive, reach concavity may be a useful metric in such settings. The middle reach of Onion Creek crossing the diapir is less concave relative to the relict upper reach and then near the downstream end of the diapir lies a more subtle knickpoint as the profile steepens

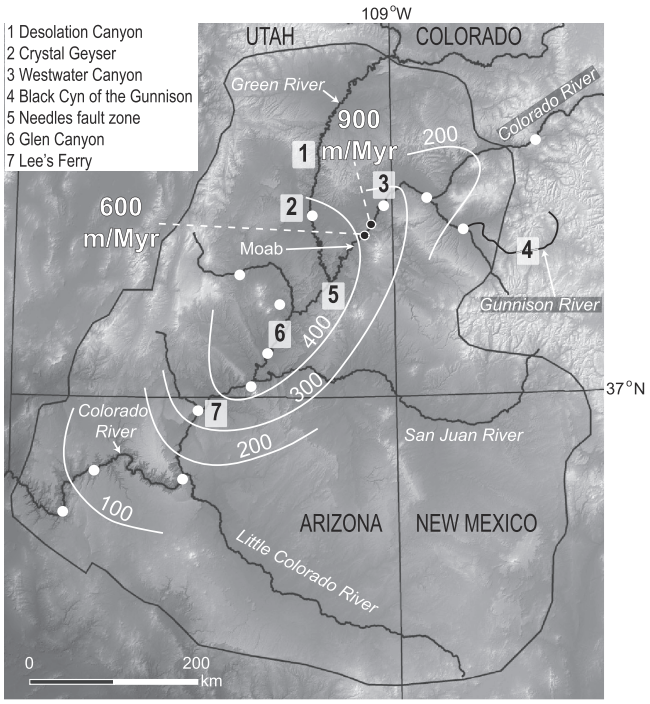

Figure 8. Colorado Plateau map showing bedrock incision rates calculated in this study (black dots with white trim) relative to the bull's eye pattern of comparable late Pleistocene bedrock incision from other studies located by white dots (modified from *Pederson et al.* [2013a]). Key locations discussed in text related to transient incision along the Colorado River system and salt deformation are also shown. Note similar drainage positions of Desolation and Westwater canyons, knickzones where we hypothesize that transient incision is partly stalled.

toward the Colorado River (Figure 6a). We suggest that this may reflect the middle reach being held up and the profile straightened by continuing uplift of the diapir since the mid-Pleistocene activity documented by *Colman* [1983]. To the south, Castle Creek has long profile patterns consistent with active subsidence of the Castle Valley graben. The high concavity of middle Castle Creek reflects the stream's transition from its steep profile in igneous rocks to low gradients through the subsiding graben (Figure 6b). Although the downstream knickpoint (kp_d) is subtle in Figure 6, it separates a middle, subsiding reach from a lower, steeper reach through Triassic strata to meet base level at the Colorado River (Figure 5). These results are frankly less definitive than anticipated, and it is logical that dissolvable salt caprock and subsiding basin fill may have a weak influence on bed resistance and stream gradient compared to other geologic controls. Still, we illustrate that concavity holds some promise as a metric for assessing activity in other settings where stream channels traverse salt structures.

5.3. Regional Drivers of Incision and Deformation

Late Pleistocene incision rates are relatively high for this region and increase upstream across the study area from ~600 m/Myr around Ida Gulch to ~900 m/Myr at Dewey Bridge (Figure 7). These are the fastest incision rates yet measured along the trunk rivers in the Colorado Plateau, given comparison to other well-dated terrace records over similar time scales [*Pederson et al.*, 2013a]. These rapid rates upstream of Moab strengthen the hypothesis that canyon-scale unloading is unleashing salt deformation. But what drives such rapid incision in lieu of active, regional tectonic uplift?

First, these high rates should partly reflect enhanced incision from broad erosional unloading and flexural rebound of the central Colorado Plateau [*Pederson et al.*, 2013a]. Yet the measured rates are ~1.5 to 2.5 times faster than that predicted for this area by the "bull's eye" hypothesis (Figure 8), and thus, other mechanisms must augment the overall rapid incision here. Second, the rapid Colorado River incision across the entire study area is not due to the more localized salt deformation, which is mostly subsidence after all. At a smaller scale, the subsidence in the Professor Valley reach does provide one hypothesis for why incision rates are higher upstream at Dewey Bridge compared to downstream at Ida Gulch. Inasmuch as the rate of local subsidence was, at certain times, greater than the rate of overall base-level fall along the river (thus causing aggradation of fill terraces in Professor Valley), and if aggradation was also too slow to maintain transport grade across the subsiding stretch, then the reach upstream would experience an additional increment of local base-level fall, though temporary. However, we prefer an alternate hypothesis that considers the greater context of the long profile. In this view, the isolated subsidence in Professor Valley was readily filled by sediment as the river maintained its transport grade and connection to the next reach downstream, as evidenced by the fill terraces we see there. Thus, subsidence only locally offsets and reduces the more rapid incision rates that exist across the broader profile due to base-level fall along the system (Figure 4).

In addition to the relatively fast rates, the apparent pattern of increasingly rapid incision upstream through the field area requires explanation. We suggest that this pattern is consistent with the wake of a transient signal, where the fastest incision has recently propagated past downstream reaches and is currently located upstream along the Colorado River. Rates in the study area also contrast with much slower but poorly constrained incision farther upstream near the Utah-Colorado border [*Aslan and Hanson*, 2009; *Pederson et al.*, 2013a]. Between these lies the Westwater Canyon knickzone (Figure 8), and this pattern of incision rates indicates that part of the propagating incision on the Colorado River is currently stalled there. Desolation Canyon, at an analogous position on the Green River upstream of Crystal Geyser, has been interpreted the same way (Figure 8) [*Pederson et al.*, 2013b]. Additionally, the transient incision recorded across the Black Canyon of the Gunnison knickzone in the Rocky Mountain headwaters is another example of such behavior, upstream of our study area along the greater Colorado River system [*Donahue et al.*, 2013]. In that case, drainage capture just downstream, along with potentially active uplift of the Rockies upstream, play roles in the differential incision—effects that are not found in our study area. Instead, the apparent wave of incision passing through our study area upstream of Moab could potentially be part of the original base-level fall from the Colorado River's integration off the plateau ~1000 km downstream at the west end of Grand Canyon [*Pederson and Tressler*, 2012]. *Cook et al.* [2009] and *Darling et al.* [2012] also recognize this ultimate source of base-level fall for their Glen Canyon localities in the central plateau, but they also interpret a shift to faster incision upstream of the Lee's Ferry knickpoint ~500 ka, generated by an unknown base-level fall. Perhaps the faster incision observed in our study area several hundred kilometers upstream represents this more recent and not yet understood transient signal.

Contrary to the expectations of the first geoscientists here and many since, the central Colorado Plateau illustrates the dynamic landscape evolution possible in regions far from plate margins and from sources of traditional tectonic uplift. Instead of impulsive uplift of unknown source [*Powell*, 1875; *Davis*, 1901] or differential mantle-driven uplift [*Karlstrom et al.*, 2012], the rapid incision and deformation documented in this case study are ultimately driven by base-level fall millions of years ago and far downstream in Grand Canyon. Then as erosion has propagated headward across hundreds of kilometers of the central plateau, it has set loose feedback from the regional dome of isostatic rebound as well as more localized salt deformation.

6. Conclusions

1. Dated and correlated Colorado River terraces reveal patterns of deformation involving thickening of deposits and deformation of straths across the study reaches, with ~500 m/Myr of time-integrated subsidence in Professor Valley. This may be the result of salt being siphoned at the surface from the neighboring Onion Creek diapir and the Cache Valley salt wall, driving salt movement at depth, creating the elliptical bowl of Professor Valley.
2. Subtle patterns of k_{sn} and especially concavity in local Colorado River tributaries are consistent with more recent uplift of the Onion Creek diapir and ongoing subsidence of the Castle Valley graben. This is a first effort to use such metrics with salt tectonics, and it illustrates modest potential.
3. Salt deformation is more active than previously thought in the study area and represents a control on fluvial sedimentation that has both modern and ancient analogues worldwide. Calculation of rapid Colorado River incision supports a connection between canyon-scale erosional unloading and salt deformation as hypothesized by previous workers.
4. Increasingly rapid late Pleistocene bedrock incision upstream along the Colorado River through the study area, from ~600 at Ida Gulch to 900 m/Myr at Dewey Bridge (the fastest rate yet measured in the Colorado Plateau), may reflect the wake of transient incision. This could have originated ~6 Ma with the integration of the Colorado River off the Colorado Plateau far downstream in Grand Canyon, or it may relate to a younger pulse of incision of unknown source. The pattern of rapid incision below and much slower incision above major knickzones of the northcentral plateau indicates that transient incision is now partly hung up in Westwater and Desolation canyons.
5. Despite there being no known or hypothesized sources of active, traditional tectonic uplift, this study area in the central Colorado Plateau reveals dynamic landscape evolution, providing a case study of a transient landscape where incision and deformation are controlled by local bedrock geology and isostatic feedback to erosion.

Acknowledgments
The data presented in this paper and additional information are available in the MS thesis of A. Jochems, which can be downloaded at http://digitalcommons.usu.edu/etd/1754/. Support was provided to A. Jochems through the Peter R. McKillop Scholarship awarded by the Department of Geology, Utah State University. We thank Tammy Rittenour and Michelle Nelson of the USU Luminescence Laboratory for their expertise and training with geochronology samples. Suggestions from Associate Editor Nicole Gasparini and three anonymous reviewers greatly improved this manuscript.

References

Aslan, A., and P. Hanson (2009), Late Pleistocene Colorado River terraces, western Colorado: A test of the stream power model (abstract), Geol. Soc. Am. Abstr. Programs, 41(7), 622.

Balco, G., and J. O. H. Stone (2005), Measuring middle Pleistocene erosion rates with cosmic-ray-produced nuclides in buried alluvial sediment, Fisher Valley, southeastern Utah, *Earth Surf. Processes Landforms*, *30*(8), 1051–1067, doi:10.1002/esp.1262.

Bull, W. B. (1990), Stream-terrace genesis: Implications for soil development, *Geomorphology*, *3*, 351–367, doi:10.1016/0169-555X(90)90011-E.

Burbank, D. W., J. Leland, E. Fielding, R. S. Anderson, N. Brozovic, M. R. Ried, and C. Duncan (1996), Bedrock incision, rock uplift and threshold hillslopes in the northwestern Himalayas, *Nature*, *379*, 505–510.

Case, J. E., and H. R. Joesting (1972), Regional geophysical investigations in the central Colorado Plateau, *U.S. Geol. Surv. Prof. Pap.*, 736, 31 pp.

Cater, F. (1970), Geology of the salt anticline region in southwestern Colorado, *U.S. Geol. Surv. Prof. Pap.*, *637*, 80 pp.

Colman, S. M. (1983), Influence of the Onion Creek salt diapir on the late Cenozoic history of Fisher Valley, southeastern Utah, *Geology*, *11*(4), 240–243.

Cook, K. L., K. X. Whipple, A. M. Heimsath, and T. C. Hanks (2009), Rapid incision of the Colorado River in Glen Canyon: Insights from channel profiles, local incision rates, and modeling of lithologic controls, *Earth Surf. Processes Landforms*, 994–1010, doi:10.1002/esp.1790.

Darling, A. L., K. E. Karlstrom, D. E. Granger, A. Aslan, E. Kirby, W. B. Ouimet, G. D. Lazear, D. D. Coblentz, and R. D. Cole (2012), New incision rates along the Colorado River system based on cosmogenic burial dating of terraces: Implications for regional controls on Quaternary incision, *Geosphere*, *8*(5), 1020–1041.

Davis, W. M. (1901), An excursion to the Grand Canyon of the Colorado, *Bull. Mus. Comp. Zool., Harvard College*, *38*(4), 107–201.

Doelling, H. H. (1996), Geologic map of the Dewey quadrangle, Grand County, Utah, *Utah Geol. Surv. Map*, *169*.

Doelling, H. H. (2001), Geologic map of the Moab and eastern part of the San Rafael Desert 30′ × 60′ quadrangles, Grand and Emery Counties, Utah, and Mesa County, Colorado, *Utah Geol. Surv. Map*, *180*.

Doelling, H. H. (2002), Geologic map of the Fisher Towers quadrangle, Grand County, Utah, *Utah Geol. Surv. Map*, *183*.

Doelling, H. H., and M. L. Ross (1998), Geologic map of the Big Bend quadrangle, Grand County, Utah, *Utah Geol. Surv. Map*, *171*.

Doelling, H. H., C. G. Oviatt, and P. W. Huntoon (1988), Salt deformation in the Paradox Basin, *Utah Geol. Min. Surv. Bull.*, *122*, 93 pp.

Donahue, M. S., K. E. Karlstrom, A. Aslan, A. Darling, D. Granger, E. Wan, R. G. Dickinson, and E. Kirby (2013), Incision history of the Black Canyon of Gunnison, Colorado, over the past 1 Ma inferred from dating of fluvial gravel deposits, *Geosphere*, *9*(4), 815–826.

Finnegan, N. J., and G. Balco (2013), Sediment supply, base level, braiding, and bedrock river terrace formation: Arroyo Seco, California, USA, *Geol. Soc. Am. Bull.*, *125*(7/8), 1114–1124, doi:10.1130/B30727.1.

Finnegan, N. J., R. Schumer, and S. Finnegan (2014), A signature of transience in bedrock river incision rates over time scales of 10^4–10^7 years, *Nature*, *505*, 391–394, doi:10.1038/nature12913.

Flint, J. J. (1974), Stream gradient as a function of order, magnitude, and discharge, *Water Resour. Res.*, *10*(5), 969–973, doi:10.1029/WR010i005p00969.

Flowers, R. M., B. P. Wernicke, and K. A. Farley (2008), Unroofing, incision, and uplift history of the southwestern Colorado Plateau from apatite (U-Th)/He thermochronometry, *Geol. Soc. Am. Bull.*, *120*(5–6), 571–587.

Frankel, K. L., and F. J. Pazzaglia (2006), Mountain fronts, base-level fall, and landscape evolution: Insights from the southern Rocky Mountains, in *Tectonics, Climate, and Landscape Evolution: Geological Society of America Special Paper 398: Penrose Conference Series*, edited by S. Willett et al., pp. 419–434, Geol. Soc. of Am., Boulder, Colo.

Furuya, M., K. Mueller, and J. Wahr (2007), Active salt tectonics in the Needles District, Canyonlands (Utah) as detected by interferometric synthetic aperture radar and point target analysis: 1992–2002, *J. Geophys. Res.*, *112*, B06418, doi:10.1029/2006JB004302.

Galbraith, R. F., R. G. Roberts, G. M. Laslett, H. Yoshida, and J. M. Olley (1999), Optical dating of single and multiple grains of quartz from Jinmium rock shelter, northern Australia: Part I, Experimental design and statistical models, *Archaeometry*, *41*(2), 339–364.

Gardner, T. W., D. W. Jorgensen, C. Shuman, and C. R. Lemieux (1987), Geomorphic and tectonic process rates: Effects of measured time interval, *Geology*, *15*, 259–261.

Guérin, G., N. Mercier, and G. Adamiec (2011), Dose-rate conversion factors: Update, *Ancient TL*, *29*(1), 5–8.

Guerrero, J., F. Gutiérrez, and P. Lucha (2008), Impact of halite dissolution subsidence on Quaternary fluvial terrace development: Case study of the Huerva River, Ebro Basin, NE Spain, *Geomorphology*, *100*(1–2), 164–179, doi:10.1016/j.geomorph.2007.04.040.

Guerrero, J., R. L. Bruhn, J. P. McCalpin, F. Gutierrez, G. Willis, and M. Mozafari (2015), Salt-dissolution faults versus tectonic faults from the case study of salt collapse in Spanish Valley, SE Utah (USA), *Lithosphere*, *7*(1), 46–58, doi:10.1130/L385.1.

Gustavson, T. C. (1986), Geomorphic development of the Canadian River Valley, Texas Panhandle: An example of regional salt dissolution and subsidence, *Geol. Soc. Am. Bull.*, *97*, 459–472.

Gutiérrez, F. (1996), Gypsum karstification induced subsidence: Effects on alluvial systems and derived geohazards (Calatayud Graben, Iberian Range, Spain), *Geomorphology*, *16*, 277–293.

Gutiérrez, F. (2004), Origin of the salt valleys in the Canyonlands section of the Colorado Plateau, *Geomorphology*, *57*(3–4), 423–435, doi:10.1016/S0169-555X(03)00186-7.

Gutiérrez, F., D. Carbonel, R. M. Kirkham, J. Guerrero, P. Lucha, and V. Matthews (2014), Can flexural-slip faults related to evaporite dissolution generate hazardous earthquakes? The case of the Grand Hogback monocline of west-central Colorado, *Geol. Soc. Am. Bull.*, *126*(11–12), 1481–1494, doi:10.1130/B31054.1.

Hack, J. T. (1973), Stream-profile analysis and stream-gradient index, *J. Res. U.S. Geol. Surv.*, *1*, 421–429.

Hancock, G. S., and R. S. Anderson (2002), Numerical modeling of fluvial strath-terrace formation in response to oscillating climate, *Geol. Soc. Am. Bull.*, *114*, 1131–1142.

Hazel, J. E., Jr. (1994), Sedimentary response to intrabasinal salt tectonism in the Upper Triassic Chinle Formation, Paradox Basin, Utah, *U.S. Geol. Surv. Bull.*, *2000-F*, pp. F1-F44.

Hoffman, M., D. F. Stockli, S. A. Kelley, J. Pederson, and J. Lee (2011), Mio-Pliocene erosional exhumation of the central Colorado Plateau, eastern Utah: New insights from apatite (U-Th)/He thermochronometry, in *CREvolution 2—Origin and Evolution of the Colorado River*, *U.S. Geol. Surv. Open-File Rep.*, *2011-1210*, pp. 132–136.

Howard, A. (1994), A detachment-limited model of drainage basin evolution, *Water Resour. Res.*, *30*, 2261–2285, doi:10.1029/94WR00757.

Huntley, D. J., D. I. Godfrey-Smith, and M. L. W. Thewalt (1985), Optical dating of sediments, *Nature*, *313*, 105–107.

Huntoon, P. W. (1982), The Meander anticline, Canyonlands, Utah: An unloading structure resulting from horizontal gliding on salt, *Geol. Soc. Am. Bull.*, *93*, 941–950.

Jerolmack, D. J., and C. Paola (2010), Shredding of environmental signals by sediment transport, *Geophys. Res. Lett.*, *37*, L19401, doi:10.1029/2010GL044638.

Jochems, A. P. (2013), Formation, deformation, and incision of Colorado River terraces upstream of Moab, Utah, MS thesis, 193 pp., Utah State Univ., Logan.
Karlstrom, K. E., R. Crow, L. J. Crossey, D. Coblentz, and J. W. van Wijk (2008), Model for tectonically driven incision of the younger than 6 Ma Grand Canyon, *Geology*, *36*, 835–838.
Karlstrom, K. E., et al. (2012), Mantle-driven dynamic uplift of the Rocky Mountains and Colorado Plateau and its surface response: Toward a unified hypothesis, *Lithosphere*, *4*(1), 3–22, doi:10.1130/L150.1.
Kirby, E., and K. X. Whipple (2012), Expression of active tectonics in erosional landscapes, *J. Struct. Geol.*, *44*, 54–75, doi:10.1016/j.jsg.2012.07.009.
Kirkham, R. M., R. K. Streufert, M. J. Kunk, J. R. Budahn, M. R. Hudson, and W. J. Perry Jr. (2002), Evaporite tectonism in the lower Roaring Fork River valley, west-central Colorado, in *Late Cenozoic Evaporite Tectonism and Volcanism in West-Central Colorado*, edited by R. M. Kirkham, R. B. Scott, and T. W. Judkins, *Geol. Soc. Am. Spec. Pap.*, *366*, 73–99.
Lazear, G., K. Karlstrom, A. Aslan, and S. Kelley (2013), Denudation and flexural isostatic response of the Colorado Plateau and southern Rocky Mountains region since 10 Ma, *Geosphere*, *9*(4), 792–814.
Lee, J. P., D. F. Stockli, S. A. Kelley, J. L. Pederson, K. E. Karlstrom, and T. A. Ehlers (2013), New thermochronometric constraints on the Tertiary landscape evolution of the central and eastern Grand Canyon, Arizona, *Geosphere*, *9*(2), 216–228.
Levander, A., B. Schmandt, M. S. Miller, K. Liu, K. E. Karlstrom, R. S. Crow, C.-T. A. Lee, and E. D. Humphreys (2011), Continuing Colorado plateau uplift by delamination-style convective lithospheric downwelling, *Nature*, *472*, 461–465, doi:10.1038/nature10001.
Merritts, D. J., K. R. Vincent, and E. E. Wohl (1994), Long river profiles, tectonism, and eustasy: A guide to interpreting fluvial terraces, *J. Geophys. Res.*, *99*(B7), 14,031–14,050, doi:10.1029/94JB00857.
Merritts, D.J., and M. Ellis, eds. (1994), Tectonics and topography, *Special Issue J. Geophys. Res.*, *99*(B6), 12,135–12,315, 13,871–14,050, 20,063–20,321, doi:10.1029/94JB00180.
Molnar, P., and P. England (1990), Late Cenozoic uplift of mountain ranges and global climate change: Chicken or egg?, *Nature*, *346*, 29–34.
Montgomery, D. R. (2004), Observations on the role of lithology in strath terrace formation and bedrock channel width, *Am. J. Sci.*, *304*, 454–476, doi:10.2475/ajs.304.5.454.
Moucha, R., A. M. Forte, D. B. Rowley, J. X. Mitrovica, N. A. Simmons, and S. P. Grand (2009), Deep mantle forces and the uplift of the Colorado Plateau, *Geophys. Res. Lett.*, *36*, L19310, doi:10.1029/2009GL039778.
Murray, A. S., and A. G. Wintle (2000), Luminescence dating of quartz using an improved single-aliquot regenerative-dose protocol, *Radiat. Meas.*, *32*, 57–73.
Murray, A. S., and J. M. Olley (2002), Precision and accuracy in the optically stimulated luminescence dating of sedimentary quartz: A status review, *Geochronometria*, *21*, 1–16.
Pazzaglia, F. J. (2013), 9.22 Fluvial terraces, in *Treatise on Geomorphology*, edited by J. F. Shroder, pp. 379–412, Academic Press, San Diego, Calif.
Pazzaglia, F. J., and M. T. Brandon (2001), A fluvial record of long-term steady state uplift and erosion across the Cascadia forearc high, western Washington State, *Am. J. Sci.*, *301*, 385–431.
Pazzaglia, F. J., and P. L. K. Knuepfer (2001), The steady state orogen: Concepts, field observations, and models, *Am. J. Sci.*, *302*, 313–512.
Pederson, J. L., and C. Tressler (2012), Colorado River long-profile metrics, knickzones and their meaning, *Earth Planet. Sci. Lett.*, *345-348*, 171–179, doi:10.1016/j.epsl.2012.06.047.
Pederson, J. L., R. D. Mackley, and J. L. Eddleman (2002), Colorado Plateau uplift and erosion evaluated using GIS, *Geol. Soc. Am.*, *12*(8), 4–10.
Pederson, J. L., M. D. Anders, T. M. Rittenour, W. D. Sharp, J. C. Gosse, and K. E. Karlstrom (2006), Using fill terraces to understand incision rates and evolution of the Colorado River in eastern Grand Canyon, Arizona, *J. Geophys. Res.*, *111*, F02003, doi:10.1029/2004JF000201.
Pederson, J. L., W. S. Cragun, A. J. Hidy, T. M. Rittenour, and J. C. Gosse (2013a), Colorado River chronostratigraphy at Lee's Ferry, Arizona, and the Colorado Plateau bull's-eye of incision, *Geology*, *41*(4), 427–430, doi:10.1130/G34051.1.
Pederson, J. L., N. Burnside, Z. Shipton, and T. M. Rittenour (2013b), Rapid river incision across an inactive fault—Implications for patterns of erosion and deformation in the central Colorado Plateau, *Lithosphere*, *5*, 513–520.
Powell, J. W. (1875), Exploration of the Colorado River of the West and its tributaries, 1869–1872, Smithsonian Institute Annu. Rep., 291 pp.
Prince, P. S., J. A. Spotila, and W. S. Henika (2011), Stream capture as driver of transient landscape evolution in a tectonically quiescent setting, *Geology*, *39*(9), 823–826, doi:10.1130/G32008.1.
Rittenour, T. M. (2008), Luminescence dating of fluvial deposits: Applications to geomorphic, paleoseismic and archaeological research, *Boreas*, *37*, 613–635, doi:10.1111/j.1502-3885.2008.00056.x.
Roy, M., T. H. Jordan, and J. Pederson (2009), Colorado Plateau magmatism and uplift by warming of heterogeneous lithosphere, *Nature*, *459*, 978–982, doi:10.1038/nature08052.
Schmandt, B., and E. Humphreys (2010), Complex subduction and small-scale convection revealed by body-wave tomography of the western United States upper mantle, *Earth Planet. Sci. Lett.*, *297*, 435–445.
Schoenbohm, L. M., K. X. Whipple, B. C. Burchfiel, and L. Z. Chen (2004), Geomorphic constraints on surface uplift, exhumation, and plateau growth in the Red River region, Yunnan Province, China, *Geol. Soc. Am. Bull.*, *116*(7/8), 895–909.
Snyder, N. P., K. X. Whipple, G. E. Tucker, and D. J. Merritts (2000), Landscape response to tectonic forcing: Digital elevation model analysis of stream profiles in the Mendocino triple junction region, northern California, *Geol. Soc. Am. Bull.*, *112*(8), 1250–1263.
Strahler, A. N. (1952), Hypsometric (area-altitude) analysis of erosional topography, *Geol. Soc. Am. Bull.*, *63*, 1117–1142.
Trudgill, B. D. (2011), Evolution of salt structures in the northern Paradox Basin: Controls on evaporite deposition, salt wall growth and supra-salt stratigraphic architecture: Evolution of salt structures in the northern Paradox Basin, *Basin Res.*, *23*(2), 208–238, doi:10.1111/j.1365-2117.2010.00478.x.
van Wijk, J. W., W. S. Baldridge, J. Van Hunen, S. Goes, R. Aster, D. D. Coblentz, S. P. Grand, and J. Ni (2010), Small-scale convection at the edge of the Colorado Plateau: Implications for topography, magmatism, and evolution of Proterozoic lithosphere, *Geology*, *38*(7), 611–614.
Wegmann, K. W., and F. J. Pazzaglia (2002), Holocene strath terraces, climate change, and active tectonics: The Clearwater River basin, Olympic Peninsula, Washington State, *Geol. Soc. Am. Bull.*, *114*(6), 731–744.
Whipple, K. X. (2004), Bedrock rivers and the geomorphology of active orogens, *Annu. Rev. Earth Planet. Sci.*, *32*, 151–185.
Whipple, K. X., and G. E. Tucker (1999), Dynamics of the stream-power river incision model: Implications for height limits of mountain ranges, landscape response timescales, and research needs, *J. Geophys. Res.*, *104*(B8), 17,661–17,674, doi:10.1029/1999JB900120.
Wobus, C., K. X. Whipple, E. Kirby, N. Snyder, J. Johnson, K. Spyropoulou, B. Crosby, and D. Sheehan (2006), Tectonics from topography: Procedures, promise, and pitfalls, in *Tectonics, Climate, and Landscape Evolution: Geological Society of America Special Paper 398: Penrose Conference Series*, edited by S. Willett et al., pp. 55–74, Geol. Soc. of Am., Boulder, Colo.
Zaprowski, B. J., E. B. Evenson, F. J. Pazzaglia, and J. B. Epstein (2001), Knickzone propagation in the Black Hills and northern High Plains: A different perspective on the late Cenozoic exhumation of the Laramide Rocky Mountains, *Geology*, *29*(6), 547–550.